

Influence of Deposition Conditions on the Properties of Chemically Deposited Cu₂O Film

Dr. Ali M. Mousa* & Abdal-Satar Kuther **

Received on: 25/ 10/ 2009

Accepted on: 1/ 4/ 2010

Abstract

Cuprous oxide films have been deposited by chemical bath method from alkaline solution at pH=8.6. The deposited oxides were investigated using X-ray diffraction, surface morphology, optical and electrical measurements. It is shown that during deposition two different stages could be distinguished. The band gap of the deposited film tuned from 2eV to 2.5 eV by decreasing deposition time. X-ray diffraction (XRD) measurements showed formation of CuO and Cu₂O phases, the structure shows a thickness dependent. The grain size of as deposited and annealed films at different temperatures were calculated from SEM data, The results showed that the grain size of films increased with increasing deposition time and annealing temperature. The resistivity of the films had significantly decreased with increased deposition time, also films activation energy decreased with increasing thickness

Keywords: Cuprous oxide , CBD, X-ray diffraction, nano film

تأثير ظروف الترسيب على خصائص اوكسيد النحاس المرسب بالحام الكيميائي

الخلاصه

تم إجراء ترسيب أوكسيد النحاس من محاليل قاعدية بدرجة حامضية 8.6 . الاغشية المرسبه درست بواسطة حيود الاشعه السينيه,القياسات الكهربائيه والثياسات البصريه. ظهر أنه خلال الترسيب هنالك مرحاتين متميزتين.تغيرت قيمة فجوة الطاقه لغشاء المرسب من 2.أف الى 2.5 أف بتقليص زمن الترسيب.كذلك ظهر من انماط حيود الاشعه السينيه تكون طورين هما وأظهرت الانماط اعتماد التركيب البلوري على السمك . من خلال صور المجهر الاليكتروني الماسح تم حساب الحجم الحبيبي والتي بينت ان الحجم الحبيبي يزداد بزيادة زمن الترسيب وزيادة درجة حرارة التلدين. من القياسات Cu₂O,CuO الكهربيائيه تبين ان المقاوميه الكهربائيه تقل مع زيادة زمن الترسيب وكذلك تقل طاقه التأين مع زيادة السمك.

*Applied Sciences Department, University of Technology/Baghdad
** Ministry of Science and Technology/Baghdad

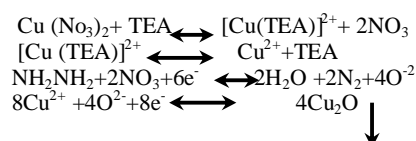
Introduction

Cu₂O is an important metal-oxide p-type semiconductor (1). The nature of the p-type is originated from the presence of Cu vacancies which form an acceptor level above the valance band (2). Cu₂O with direct band gap of about 2.1eV (3) which therefore strongly absorbs at $\lambda < 600\text{nm}$ has been regarded as one of the most promising materials used for optoelectronic applications (4,5). The theoretical energy conversion efficiency of 20% makes it possible to be used as an absorber layer in thin film heterojunctions solar cell (6). Besides the optoelectronic applications Cu₂O is a basic compound forming superconducting Materials, magnetic storage and gassensors (7,8). Several methods have been used to prepare Cu₂O including pulsed laser deposition(9), DC reactive magnetron Sputtering (10), atmospheric chemical vapour deposition(11) and chemical bath deposition(12-14). Among these, CBD is the cheapest, simplest and the most convenient method, and has frequently been used for the deposition of metal oxide films. This paper explores the advantages of using CBD technique to form Cu₂O films. The structure, optical and electrical properties of the obtained films are discussed on the basis of X-ray diffraction data. The results are discussed and compared with the reported data of other techniques.

Experimental Details

The samples studied here were thin film polycrystalline films of Cu₂O layers Prepared by CBD on commercial glass slides with dimension (1*26*76mm³) in ultrasonic bath and then the

substrates were washed with distilled water immersed for 24h in chromic acid (1g of CrO₃ in 20ml of distilled water) and finally washed again with distilled water. The aqueous solution of the optimum deposition bath was 20ml of 0.1M copper nitrate (Cu(NO₃)₂), 20ml of 0.1M Hydrazine [NH₂NH₂], and 5.5ml of 1M TriEthanolAmine (TEA) which is the complex agent. The addition of 1M (TEA) to Cu (NO₃)₂ solutions resulted in a deep blue solution. The further addition of NH₂NH₂ to the solution resulted in a hissing sound which signaled the release of Nitrogen gas and a Rapid change in color, first to light blue and then to light yellow, reddish brown, and finally blue. The solution was stirred with a magnetic stirrer. The film deposited is either pure yellow or reddish brown but gradually turns yellow with time, the following variation taken place.



In order to investigate the annealing effect on the copper oxide films, the films were prepared on five separate glass substrates under same conditions. Systematically, first sample was not annealed and other four were annealed from 100°C to 250°C in steps of 50°C during 20min. in air atmosphere. The thickness of deposited Cu₂O film is measured by optical interferometer method. This method based on interference of the light beam reflection from thin film surface and bottom (at substrate). He-Ne laser (632.8nm wave length) was used and the thickness determined using the formula (15).

$$d = \frac{\Delta x}{x} \cdot \frac{l}{2} \dots\dots (1)$$

where x : is fringe width, Δx is the distance between two fringes, and l is the wave length of laser light. The transmission and absorption spectra were measured for Cu₂O films grown on glass substrates in the spectral range of 350-1050nm using a shimadzu UV-VIS spectrophotometer. The transmission spectrum used in the calculation of the absorption coefficient (α) (16)

$$a = \frac{1}{d} \ln \frac{1}{T} \dots(2)$$

where d is the thickness of thin film and (T) is the transmission. The nature and value of band gap (E_g) was determined from the graph of $(\alpha E)^2$ versus E for the thin film. The surface morphology has been studied in this work by using Scanning Electron Microscope (SEM) type JEOL-JAPAN (JSM-5600). The average grain size was determined using software with multistage and the following relationship is applied for final calculation (17)

$$D = \frac{\sqrt{av. \text{ particle size} \times 270}}{M_p} \dots (3)$$

Where M_p is the magnification power of SEM To define the preferred orientation also to determine the nature of the growth and the structured characteristics of Cu₂O films, X- Ray diffraction was carried and the phase was determined by using the ASTM charts, using Philips PW1840. The source of X-Ray radiation has CuK α radiation ($\lambda = 1.54 \text{ \AA}$). The device has been operated at 40 Kv and 20 mA emission current,. The grain size of the polycrystalline material could

be calculated from the X-Ray spectrum by means of full width at half maximum (FWHM) method (Scherrer equation) (18)

$$G_s = \frac{fl}{\Delta \cos q} \dots\dots (4)$$

Where Δ is the full width at half maximum of the (XRD) peak appearing at the diffraction angle θ , (f) Shape factor, the value of which depends on the crystalline shape. The number of crystallite layers (N_L) which could be calculated from the equation (19):

$$N_L = \frac{d}{G_s} \dots\dots (5)$$

Where (G_s) Grain size (d) is the film thickness. *Electrical Resistivity and Hall Measurements* The electrical resistivity of Cu₂O film important parameter for all applications, generally calculated from the current-voltage measurements by

$$r = R \frac{bd}{l} \dots\dots(6)$$

Where l , b , and d are the length, width and thickness of the film respectively, R is the resistance of the film measured using two aluminum electrodes (parallel strips at 5 mm in width, separated by 5 mm) deposited on the front surface, then the conductivity can be evaluated from this equation

$$s = \frac{1}{r} \dots\dots(7)$$

Hall voltage (V_H), is setup across the sample when both electrical and magnetic field applied on the sample. Four equal distance graphite electrodes are deposited on the film, Hall coefficient (R_H) is given by (20)

$$R_H = \frac{1}{n e q} \dots\dots (8)$$

where q , is electron charge, n_c is the carrier density which is related to the Hall voltage (V_H), by the following

$$\text{equation } n_c = \frac{B}{qd} \cdot \frac{I}{V_H} \quad \dots\dots (9)$$

where d is the thickness of the film. The mobility of carrier (μ_H) is given

$$\text{by } R_H = \frac{m_H}{S} \quad \dots\dots (10)$$

where $\sigma = n_c \times q \times \mu$.

Results and Discussions:

1-Kinetics of growth

By studying the variation of film thickness with deposition conditions, the information concerning the growth mechanism could be obtained. Figure (1a) shows the variation of film thickness with deposition time at room temperature, pH=8.6 and 0.1M of Cu(NO₃)₂. It is clear that the deposition rate is much faster in the first 10min. (9.71nm/min), while for longer deposition time the rate decrease to (1.09nm/min), and since the variation in thickness at longer time is very low, so the value of 140nm at 40min. could be regarded as the terminal thickness. In the first 10min. the majority of ions will deposited, hence, the deposition rate is high, in addition, the nature of the substrate surface with the time no more the same i.e. at the first 10min. high nucleation density could be expected, thus continuous growth is facilitated. Figure (1b) shows the growth as a function of molar fraction of copper nitrate in the range 0.05M-0.2M at R.T, pH=8.6 and fixed deposition time (30min.). the growth is strongly influenced by the molarities up to 0.1M with deposition ratio of (100nm/mole), and for higher molarities the growth ratio decrease by a factor of (10). This behavior is due to the

super-saturation, where in chemical deposition route the growth mechanism may be induced by the change of super saturation. Under high super saturation (as in Cu₂O) the condensed materials vary from polycrystals to fine-grained polycrystals (21).

2- Films morphology and structure properties The characterization results of the Cu₂O films morphology deposited at different time on glass substrate by CBD technique had given in figure (2a-c). It is clear that films prepared at 5min. have small irregular structure and the substrate is not completely covered. The films was composed of small packed micro crystals, the grains are well defined spherical and of almost similar size. Increasing deposition time to 15min. figure (2b) the substrate surface is well covered by a well dispersed spherical mono particle with size ranged between (12-26) nm and shape, the image also reveals that every particle uniformly attached with many smaller particles. Agglomeration of particles accompanied a 25min. deposition time as shown in figure (2c). According to the X-ray diffraction results, the choice of deposition conditions plays a crucial role in the formation of Cu₂O. Figure (3a-d) shows the influence of deposition time on the diffractograms of deposited films. All the spectra reveal that deposited films are polycrystalline in nature. By comparing with ASTM the preferred orientation of the films change from a mixture of Cu₂O and CuO phases to a pure Cu₂O single phase as the film thickness increased. The XRD pattern of the deposited films exhibits peaks at $2\theta = 36.5^\circ$ and 40.4° it also exhibit peak corresponding to

CuO. No peaks corresponding to elemental Cu which could be attributed to the strongly bounded Cu in the formation of Cu₂O compound as in the sputtering film or nonidentified peaks (10). Upon deposition with longer time the CuO phase disappeared which is confirmed from the absence of the peak correspond to CuO. The disappearing of the CuO peak with increasing deposition time could be explained by adopting the approach of S. Rom (22) (In controlled chemical reaction with reaction species dispersed in a diluted medium (as in the present work), phase with small critical volume both nucleation and growth are easily if compared with that of a bigger critical volume) i.e. increasing deposition time accompanied by redistribution entropy in favor of Cu₂O planes.

Table (1) summarized the influence of deposition time on lattice parameters and average grain size. From the table it is clear that the average grain size of (111) plane increased with deposition time, whereas that of (200) is time independent. The increasing in the average grain size implied that the growth behavior of (111) preferred film is the typical coalescence mechanism thus, the grain of (111) with faster growth rate become larger, whereas other grains with slower growth rate are consumed. Annealing at $\geq 200^{\circ}\text{C}$ the film converted completely to CuO as shown in figure (4 a, b), the conversion is results from the diffusion of Oxygen into the films, Cu₂O starts reacting with O₂ and form CuO phase according to the following reaction $2 \text{Cu}_2\text{O} + \text{O}_2 \rightarrow 4\text{CuO}$

Also annealing increasing crystallite size from 16nm to 24nm which is in agreement with reported results (24).

2-Optical properties The predomination of Cu₂O phases with increasing thickness can also be shown by the determination of the optical band gap. The optical band gap of films materials illustrated in figure (5). The curves shows that all deposited films reveals an increase in Transmission in visible region and some saturation takes place at infrared region. Decreasing deposition time (decreasing thickness) shows faster saturation and high transmission. Also, from the curve at about ($\lambda=500\text{nm}$) transmission onset is evident. Blue shift of the transmission onset is observed upon thickness decreasing, indicating rather small decreasing in the average grain size and in principle it would be expected to reflect in the increase of band gap as well. In the fundamental absorption region the optical absorption coefficient (α) was evaluated. Figure (6) shows the effect of deposition time on spectral absorption coefficient. On the basis of the optical absorption spectra using the well known relation $\alpha h\nu = A (h\nu - E_g)^n$ where A is constant, $h\nu$ is the photon energy n depending on the nature of transition, $n=1/2$ or $3/2$ for direct interband transitions allowed and forbidden respectively. The best fit of the experimental curve was obtained for $n=1/2$. The calculated values of the direct optical band gap varies with deposition time as in figure (7). The value of 2eV is close to the published in the case of thick films (3), while for thin films ($d < 100\text{nm}$) it is increased to 2.5eV. This increasing due to size quantization effect accompanying crystal size

decrease below certain limiting size. Upon annealing at temperature greater than 200°C, the sifted optical band gap is observed (1.3 eV), indicating a change in the deposition films phase to CuO, which is in agreement with the results of Necini Serin (23).

3-Electrical properties

The measured electrical resistivity of the as deposited films are in the order of (10^3 – 10^4 Ωcm), a similar results have been reported by earlier work (24). Figure (8) shows the variation of resistivity as a function of deposition time. The improvement in the electrical properties was accompanied by an improvement in the degree of film crystallinity and an increase in the grain size. The resistivity of nano crystalline film (<10min.) had a high value (10^6 – $3*10^6$ Ωcm) compared to standard films where resistivity not exceed (10^4 Ωcm), and this mainly due to the small crystallite size.

A plot of log conductivity versus inverse temperature is shown in figure (9 a,b). The linear dependence indicating the presence of only one type of conduction mechanism in the films. Our experimental data fit into the relation $\sigma = \sigma_0 \exp(-E_a/kT)$ Where σ is the conductivity at temperature T, σ_0 is constant, k is Boltzman constant, T is the absolute temperature and E_a is the activation energy given by 0.172 slope. The calculated value of the activation energy (0.53eV–0.68eV) for non nano size films and (0.76eV – 0.88eV) for nano size films.

Hall measurements indicating the p-type conductivity, figure (10 a,b) shows that the hole mobilities increased with deposition time, and this mainly due to the increasing in grain size, however, Carrier

mobility's decreased with increasing ath Concentration as shown in (b) and this because carriers generated in Conjunction with ionized defects, will serve as scattering centers and reduce mobility. conjunction with ionized defects, will serve as scattering centers and reduce mobility.

4-Conclusions

Following conclusions can be drawn from above detailed structural, electrical and optical characterization - Cuprous oxide have been successfully deposited by CBD on glass substrare. The effect of deposition time, Cuppor salt concentration have been investigated started by studying the growth dynamics, structer, optical and electrical properties.

- SEM images indicated that the film is composed of densely packed spherical micro crystals.
- Depending on deposition time the deposited materials are either with mixed phase for small deposition time and of pure single Cu₂O phase for higher deposition time. The grain size values were found to be in the range of 8-24 nm. For (1110) plane.
- optical band gap of the films was found to vary from 2 to 2.5 eV. An obvious blue shift of the near band gap absorption is observed for the nanosized Cu₂O films deposited with small deposition time, which could attributed to the quantum confinements effects.
- It has been observed that Dark DC resistivity for thin film comes out to be (10^3 – 10^4 Ωcm) and (10^6 – $3*10^6$ Ωcm) for nanofilm. -. activation energy values were found to be (0.53eV–0.68eV) and (0.76eV – 0.88eV) respectively for thin and nano film increased with optical band gap The optical and electrical

results are consistent with the X-ray diffraction results.

References

- [1]-I.Grozdanov; Mater.Lett. 19, (1994), 281.
- [2]Y.L.Liu,Y.C.Liu,R.Mv,H.Yang,C.L.Shao,J.Y.Zhang,Y.M.Lu,D.Z.Shen,X.W.fan; Semicond.Sci.Technol.20,(2005),4
- [3]-A.Merizzi, M.Masse, E.Fortin; Solid StateCommun. (2000),419.
- [4]-K.Borgohain, N.Murase, S.Mahamuni; J.Appl.Phys.92, (2002),1292.
- [5]-Y.Okamoto, S.Ishizuka, T.Sakarain, N.Fujiwara, H.Kobayashi, K.Akimmoto; Appl.Phys.Lett. 82,(2003),1060.
- [6]-T.Minami, H.Tanka, T.Shimakawa, T.Miyata, H.Sato; Japan.J.Appl.Phys 43,(2002), L917.
- [7]-W.Wang, G.Wang, X.Wang, Y.Zhan, Y.Lin,C.Zhang;adv.Mater 14,(2002),67.
- [8]-L.Gou, C.J.Murphy; NanoLetters; 3,(2003),231.
- [9]-H.kim, J.S.Horwitz, A.Pique, CM.Gilmore, D.B.Chrisey; Appl.Phys.A 69,(1999), S447.
- [10]- T. Itoh, K. Maki ; Vacuum 81 (2007) 904–910.
- [11]-Y.Matsui, .Yamamoto, S.Takeda; Mat.Res.Soc.SympProcess4, (2000),621.
- [12]-F.I.Ezema; Greenwich journal of Science and Technology; 3,(2003),110.
- [13].Tanusevski;Semicond.Sci.Tech nol. 18,(2003),501.
- [14]- S. M. Aljawad,"Physical Properties of CdS Prepared By Chemical Path Deposition"Ph.D. Thesis, Applied Science Dept., co University Of Tehnnonlogy, 2007.
- [15]- E. Pentia, L. Pintilie, V. Draghia, and M. Lisca, Balkan Physical Union, Vol.5, 2003.
- [16]- H. Reiss, P. Mirabel, and R. L. Whetten, J. Phys. Chem., Vol.92, ,(1988),7241-7246.
- [17]- R. A. Street, S. E. Ready, F. Lemmi, K. S. Shah, P. Bennelt, and, Y. Dmitrigev, Journal of Applied Physics, Vol.86, No.5, (1999),2660-2667.
- [18]- M. Yin, C. K. Wu, Y. Lou, C. Burda, and J. T. Koberstein, J. Am. Chem. Soc., Vol.127, (2005) ,9506-9511.
- [19]- B. Jordienko, Yu. N. Zhuravlev, and D. G. Fedarov, Physics of The Solid State, Vol.49, No.2, 2007, 223-228.
- [20]- A. E. Bianchi, S.J. Stewart, J. Punte, R. Vina, and I. L. Torriani; Physic A B 389, (2007), 135-139.
- [21]- G. Hodes, "Chemical Solution Deposition of Semiconductor Films", Marcel Dekker (2003).
- [22]- S. Rom, and C. Mitra, Material Science and Engineering, A 304-306, (2001), 805-809.
- [23]- N. Serin, T. Serin, S.Horzum and Y. Celik; Semicond. Sci. Technol. 20 (2005) 398–401.
- [24]- A. E. Rakhshani, Solid State Electronics, Vol.29, No.1, (1986) , 7-17.

Table (1) Analysis of the XRD study of deposited Cu₂O films

Deposition condition		plane	2 θ (degree)	FWHM (degree)	Grain size (nm)	No. of layer	d(nm) ASTM	d(nm) XRD	a(Å) ASTM	a(Å) XRD
Concentration 0.1 M Room Temperature	50min	111	37.1	0.357	24	4	2.44	2.41	4.24	4.18
		200	41.4	0.714	12	7	2.12	2.17	4.24	4.34
	45min	111	36.5	0.642	13.5	5	2.44	2.45	4.24	4.25
		200	40.4	1.07	8	7	2.12	2.22	4.24	4.44
	30min	111	36.4	0.714	13	7	2.44	2.45	4.24	4.25
		200	42	0.714	14.5	7	2.12	2.051	4.24	4.32
	15min	111	36.2	0.714	8.5	7	2.44	2.47	4.24	4.27
		200	41.5	0.714	8	7	2.12	2.17	4.24	4.34

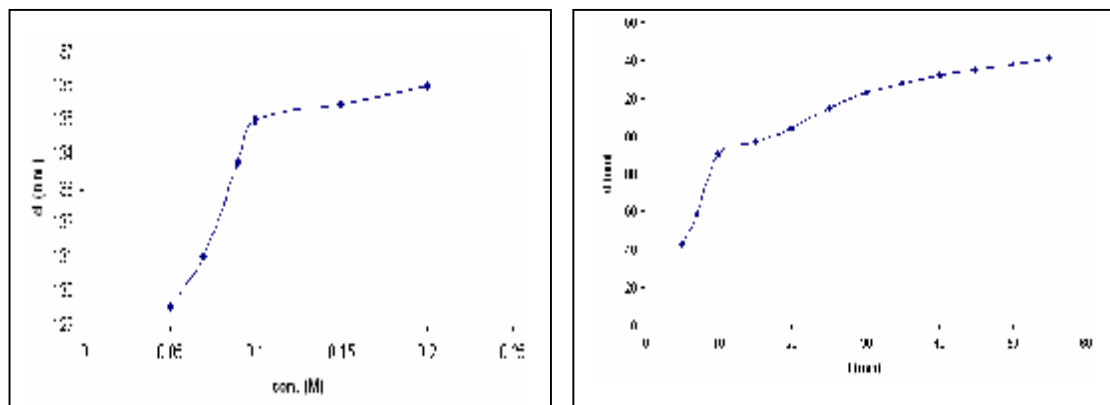


Figure (1 a , b)

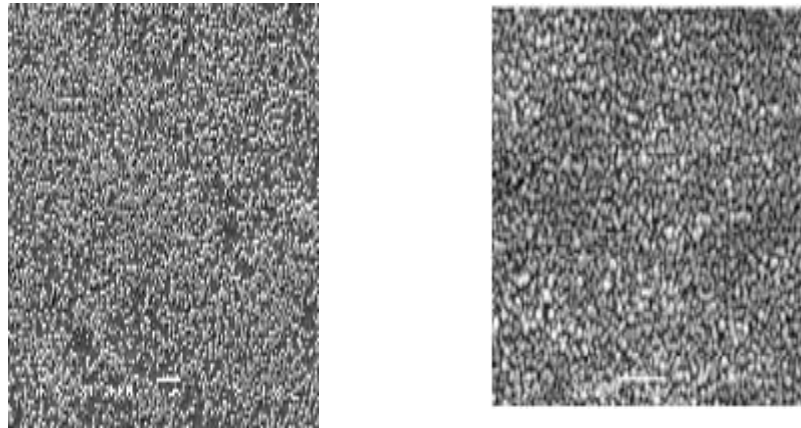


Figure (2 a-c)

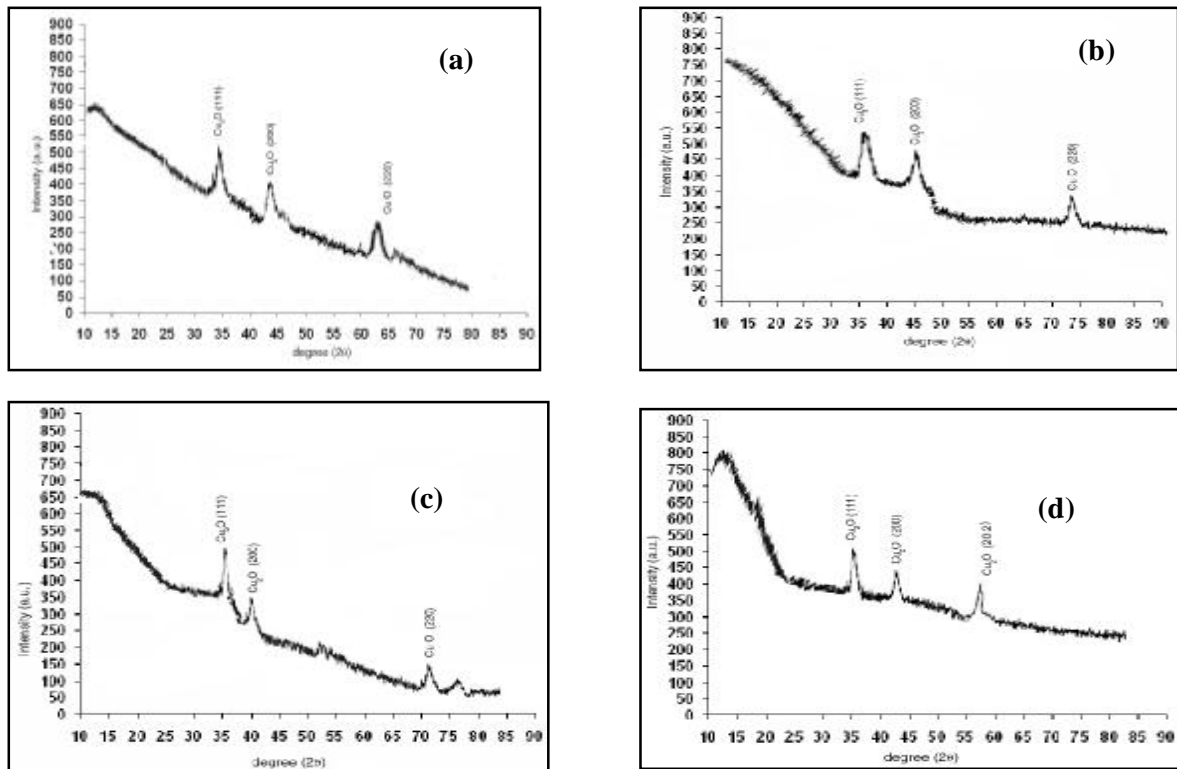


Figure (3 a - d)

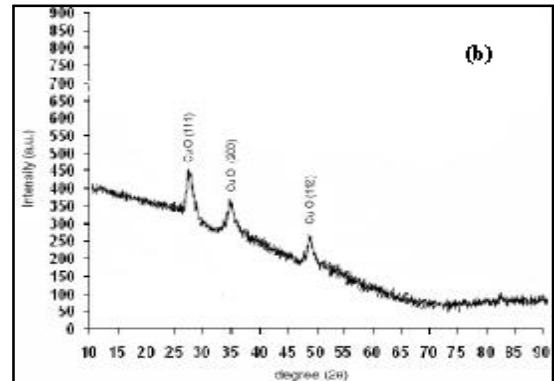
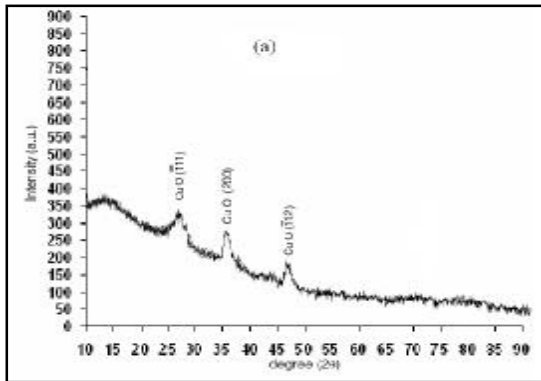


Figure (4.a,b)

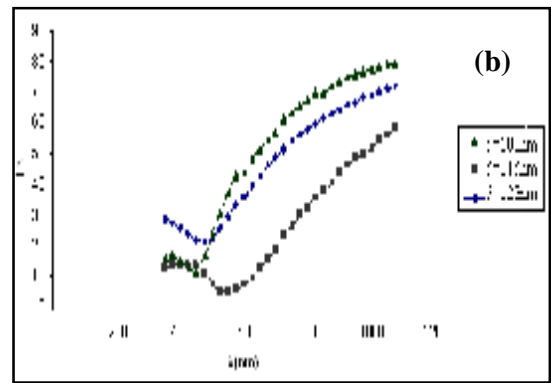
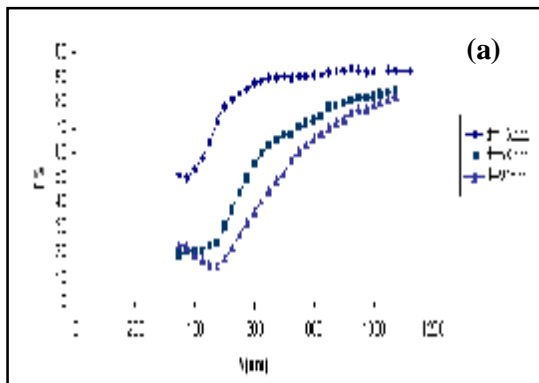


Figure (5 a,b)

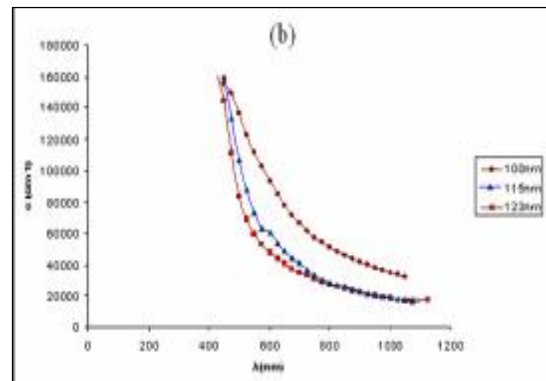
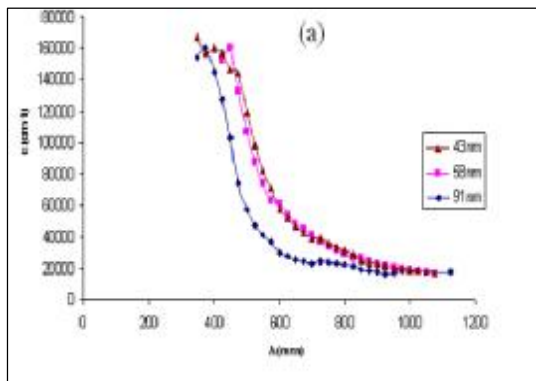


Figure (6a, b)

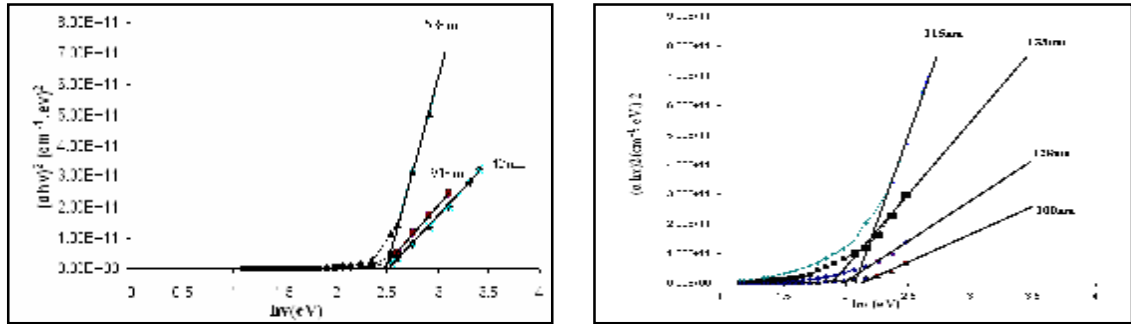


Figure (7 a,b)

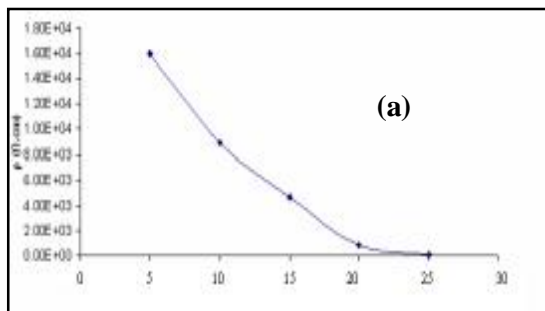


Figure (8)

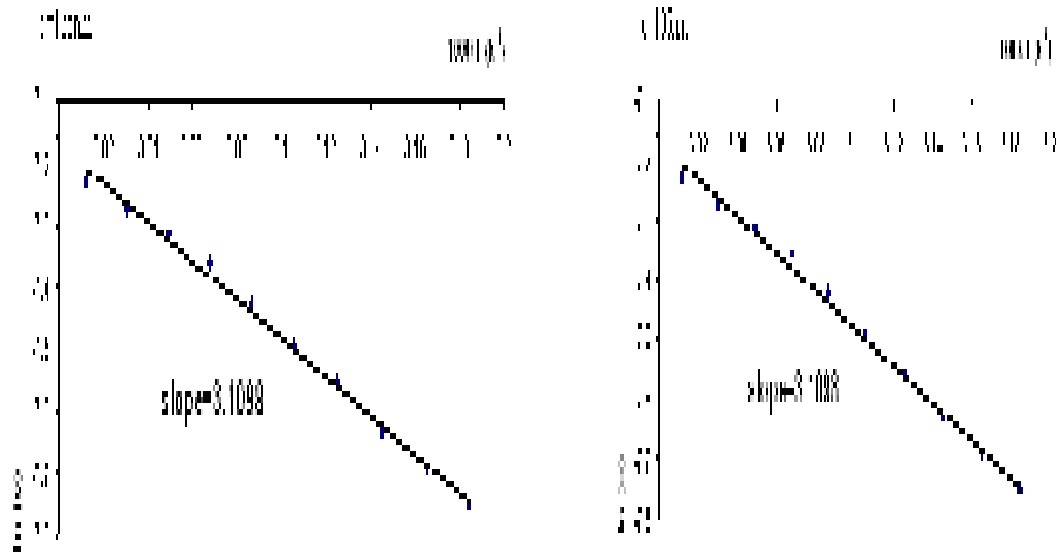
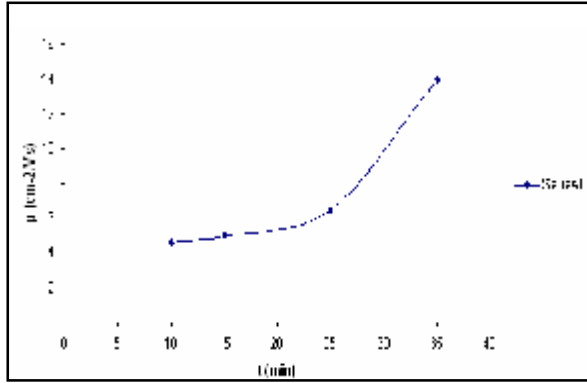
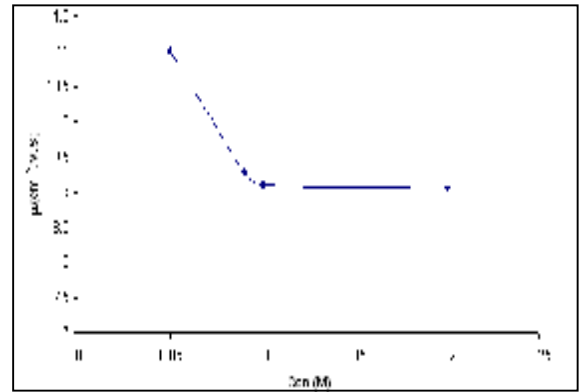


Figure (9 a,b)



(a)



(b)

Figure (10 a,b)